

Guaranteed behaviour of shape memory alloys: After quench and long time effects in CuZnAl SMA

A. Isalgue and V. Torra

CIRG, Dep. Física Aplicada UPC, Campus Nord B-4, 08034 Barcelona, Spain

Abstract: The use of Shape Memory Alloys (SMA) in critical "high tech" applications such as robotics and in continuous actuators needs an increased reliability and a guaranteed behaviour lasting several years. High resolution measurements enabled to quantify the time effects of aging near room temperature on the properties of CuZnAl SMA and to modelize the macroscopic behaviour. Some structural measurements showed small changes on the material structure.

1. INTRODUCTION

Shape memory alloys (SMA) can be considered as smart materials because of their singular thermomechanical characteristics [1], due to a thermoelastic phase transformation [2]. Long time applications, as well as work as continuous actuators, relates a strictly time guaranteed characteristics and behaviour. The warranty needs a controlled (or null) variance of properties in the coexistence of phases, and as a function of time and temperature.

The parent phase and the martensite are metaestable phases because they are obtained by quenching from high temperature [2]. This supposes an intrinsic evolving capacity, depending on the estate of the material, and the temperature and time scales, showing an apparently pseudoestochastic (but deterministic) behaviour as a result of the effect of time and room temperature variable conditions. The work of Buffard [3] established the procedures to obtain a relatively reduced variability on characteristics (transformation temperature $M_s \pm 2$ K in one year) in determined cases. Reliability of the SMA materials needs the characterisation and understanding of the evolutive processes, in order to achieve improvements of the behaviour. The characterisation of the evolutive processes needs a very accurate control of the conditions and a high resolution to establish the experimental behaviour, and eventually to modelize it.

From the experiments it can be established that there are several kinds of evolution in SMA [4]:

a) There are after quench effects, evident during some hours or days, but that can last months or years at room temperature). These effects may be easily seen as time evolution of the properties of a single phase, for instance as a considerable estabilization of martensite if transformation is done soon after the quench [2].

b) There exist some long time effects, even in a single phase, seen for instance as "microaging" effects, which result in changes of M_s according to the time and temperature [5, 6].

c) Cycling the material from parent phase to martensite and to parent phase usually generates dislocation arrays, a mechanical effect in the coexistence of phases domain. The effect is more pronounced in polycrystals or in some stress free, temperature induced transformations, at high temperature rates [4]. These fatigue effects, which produce changes on the transformation temperatures and on the shape of the hysteresis cycle, are separable if dealing with single crystals cycled in a smooth, strictly controlled way.

d) There are coexistence of phases effects [7], even when the dislocation effects are avoided (for instance in single variant, and in single interface, transformations). The presence of the interphases and the different equilibrium conditions for the phases (for instance, the vacancy concentration) can produce time evolutions.

In this work, we focus on the after-quench and on the long time effects in beta phase. High resolution

measurements enable to quantify the aging near room temperature effects on the properties of CuZnAl SMA, allow modeling accurately the macroscopic behaviour, and provide a guide for the time scales of structural investigations.

2. EXPERIMENTAL

Several single crystals of CuZnAl were used, with compositions and electron concentration given in table I. The crystals were grown by a modified Bridgmann technique, and the homogenisation thermal treatments were 1123 K for 15 min. and room temperature water quench for the specimens studied here. Samples of near 0.5mm*1mm*20mm were cut from the single crystals for the resistance measurements.

Table I. - Alloys used: composition, electronic concentration and Ms transformation temperatures.

Alloy	Cu at%	Zn at%	Al at%	Electronic concentration (e/a)	Ms / K
a	69.2	14.6	16.2	1.48	273
b	68.3	15.3	16.3	1.48	223

Electrical resistance measurements were done with a computer-controlled device, operating continuously in a thermostated room. Careful control and programming of temperature is needed to obtain reliable results: temperature control and stability to at least 0.01°C is necessary to check for small changes in the resistance value, or to look for stability at constant temperature. The temperature control was achieved in a similar way as described in [8]. The electrical resistance was measured with the four-wire technique, and positive and negative readings of current and voltage were acquired to avoid the thermal emf effects. The intensities used were near 0.2 A. Averaging of data acquired in 256 s allowed a resolution better than 1 part in 10000 on a near 1 mΩ electrical resistances [5, 6, 9].

Neutron diffraction experiments were carried out at the D9 four-circle diffractometer of the Institut Laue-Langevin high flux reactor in Grenoble. The wavelength of 0.08344 nm was obtained with a single crystal Cu monochromator in transmission geometry, which uses the (220) planes, and was calibrated with a Ge single crystal. From the characteristics of the instrument in the configuration used, the time to measure one intense Bragg peak is some ten minutes for a good quality single crystal and normal statistics (some 3.10^5 counts). The time needed for a complete collection of the reflections available with the wavelength employed (some 500 Bragg peaks) is then of the order of a day. Therefore, the observation of structural time dependences is limited to dependences much larger than ten minutes, or around a day if the collection is limited to a few "representative" peaks, and is limited also by the availability of long times of continuous observation.

3. RESULTS AND DISCUSSION

3.1. After quench effects in beta phase

The effect of the quench type can be easily shown by high resistance measurements. In figure 1 (left) is represented the resistance (of the same single crystal sample (b)) at 295.65 K as a function of time, after quenching from 1123 K into air (TT1) and into water at 293 K (TT2). The difference in behaviour is associated to a different internal state of the sample, and to a different dislocation concentration [10]. From the results, the dislocations produced in the faster quenching of small samples, should be regarded as enhancing the vacancy diffusion, responsible for the faster evolutive behaviour in the first steps of time evolution after the quench.

Neutron diffraction was performed on single crystal samples of alloy (b), in an experiment looking at atomic order changes after the quench. We indexed the Bragg peaks with a cubic cell parameter of 0.5860 nm, equivalent to 8 unit bcc cells. Atomic ordering is revealed by the superstructure peaks [11], which had appreciable intensities compared to the peaks corresponding to the basic unit cell, as the (220) peaks. The order corresponding to type B2, with narrow (020) peaks, had intensities of the peaks near 10% of that of the fundamental peaks, and there was also L2₁ type ordering, with wider and less intense (111) peaks, showing the presence of short range ordering. The intensities of the peaks indicate a nearly fully

developed long range ordering (both B2 and L2₁). After air cooling the sample from 1023 K, there seems to be a small increase on the atomic order (increase of the relative intensity of (111) peaks, figure 1 right) with time at room temperature [12, 13]. The evolution seems to be in agreement with the fact that the time constants for the after quench evolution, obtained from calorimetric measurements, depend on the mass (or dimensions) of the sample [14], and the results on fig. 1 (left) for a thinner sample of the same alloy, 20 mm*0.5 mm² versus 2*2*2 mm³). Also, it was observed that the width of the (111) peaks is larger in the water quenched than in the air quenched samples, i.e., short range order tends to long range, or to larger domains: from 50 nm in the water quenched sample to near 100 nm in the air cooled sample.

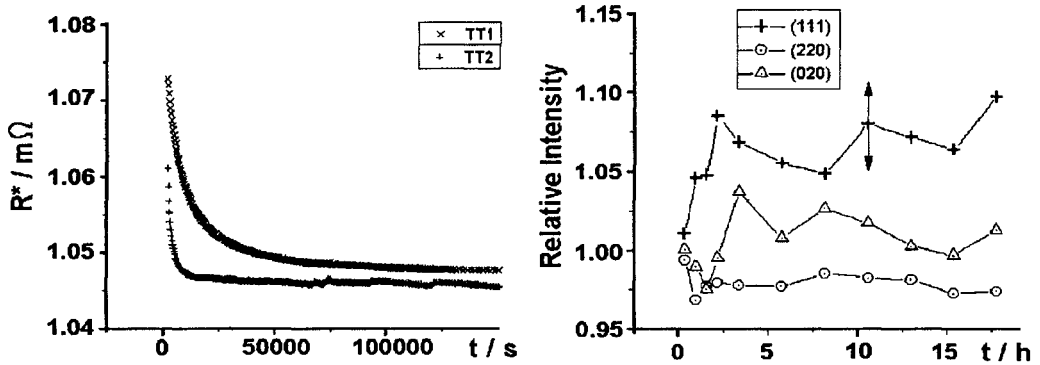


Figure 1. - Left: Resistance R^* , at 295.65 K constant temperature, as a function of time after the quench from 1123 K: x (TT1): air quenched single crystal sample; + (TT2): the same sample after water quench. Right: Relative intensity of the neutron diffraction peaks after air cooling the sample from 1073 K (single crystal composition: b). Peaks: (220) Basic structure; (020) B2 superstructure; (111) L2₁ superstructure (the arrow is an evaluation of the error). The evolution of the relative intensity of the L2₁ superstructure peak suggests a small ordering effect, presumably vacancy induced. However, the statistical errors are high to obtain more information.

3.2. Long time effects

Even long times after the quench, there remains an evolutive possibility in the alloy. This can be analyzed with a slight temperature change, as is shown in fig. 2. On one hand, from this figure, it is shown that the after quench effects remain for a long time (see, the different resistance evolutions at 389.65 K). On the other hand, even very long times after the quench, and even in cycled samples, when a temperature step is performed, the resistance evolves in a nearly exponential way to asymptotic values, with two time constants ($\tau^{(1)}$, $\tau^{(2)}$) dependent on the actual temperature of the sample [5, 6, 9]. The time constants depend on the state of the material. An asymptotic condition is early approached in some 20 thermal transformation-retransformation cycles, realised smoothly in small samples. For a thermally cycled sample of alloy (a), the first time constant $\tau^{(1)}$ is near one year at 293 K, and the second, $\tau^{(2)}$ is some three years, while at 348 K, the time constants are near 6 hours and some 4 days.

The transformation temperature M_s changes with time in a related way to the changes in resistance [5, 6]. It has been possible to modelize the M_s evolution with time and temperature. The particular effects are best visualized using $R^* = R - \beta (T - T_{ref})$, and then changes in M_s are proportional to changes in R^* . From the observed nearly exponential behaviour, the M_s time dependent value can be determined with a "tracking problem", formulated by analogy with a thermal problem, using two hidden "order" temperatures $T^{(1)}$ and $T^{(2)}$:

$$\begin{aligned} \frac{dT^{(1)}}{dt} &= - \frac{T^{(1)}(t) - T(t)}{\tau^{(1)}} \\ \frac{dT^{(2)}}{dt} &= - \frac{T^{(2)}(t) - T(t)}{\tau^{(2)}} \end{aligned} \quad (1)$$

The transformation temperature M_s can then be written: $M_s(t) = M_s(T^0) + a_1(T^{(1)}(t) - T^0) + a_2(T^{(2)}(t) - T^0)$

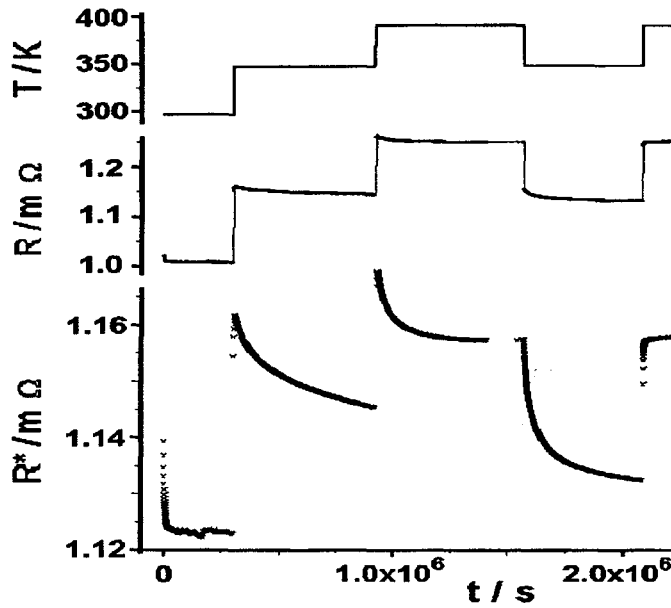


Figure 2.- From top to bottom: a) Temperature profile after water quench. b) Measured resistance. Some time evolution after the temperature steps can be detected. c) The plot of the reduced resistance $R^* = R (1 - 0.00195 \cdot (T - 348.15 \text{ K}))$ eases the detection of the time behaviour. Note that the after quench effects last more than 10^6 s at temperatures higher than 348 K (a "steady" state is reached only after nine days at 389 K)

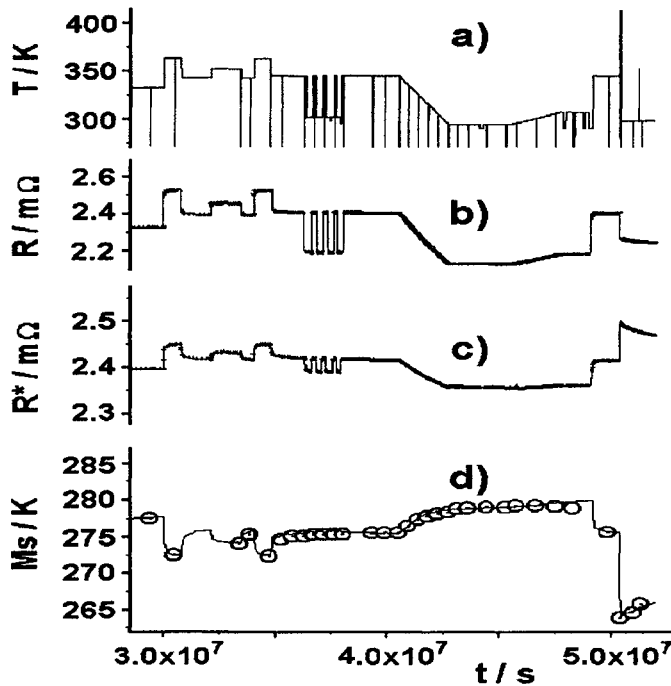


Figure 3.- Long time behaviour of alloy (a) single crystal: From top to bottom: a) Temperature profile versus time. The lines with temperature lower than 293 K correspond to the thermal cycles to measure M_s ; the electrical resistance is not represented for these processes. b) Measured resistance R . c) Reduced resistance R^* . d): (—) Computed M_s from the preceding model, and (⊙) measured M_s .

For a cycled single crystal of alloy a) from table I, it has been obtained: $\tau^{(1)} = \exp(-29.304+13630/T)$; $\tau^{(2)} = \exp(-16.933+10330/T)$; $a_1 = -0.105$; and: $a_2 = -0.067$ (where T is in K, and τ is in s).

The activation energies (1.1 eV and 0.85 eV) are higher than the vacancy formation energy. Atomic order changes [5, 15] might then be responsible for these reversible evolutions. Some new hypothesis, as a divacancy mechanism [16] might also be involved.

Some electrical resistance measurements have been done on polycrystalline Ti-51.8at%Ni, showing also an evolutive behaviour at constant temperature [9]

Some neutron diffraction experiments have been done to look for the microscopic, structural origin of the time evolution in the alloys after a temperature step. To reveal the details of the structural origin of the time evolution is desirable to have a way to improve the alloy's evolutive characteristics.

The experiments performed aimed at looking for changes in the diffraction pattern after a temperature step. If a time evolution on the intensities of the Bragg diffraction peaks is measured, then the time evolution of the atomic order would be assessed. On performing the experiments, the temperature step should be as high as possible to increase the structural effects, but not too high as fast evolutions proceed at higher temperatures, and some time is needed to measure structural parameters with enough resolution.

We performed some measurements on water quenched samples kept at 293 K during 8 months, and after characterising them at room temperature, a temperature step to 339 K was done. Some diffraction peaks, representative of the basic cubic structure, as the (220), and of the atomic order $L2_1$, corresponding to (111) and (-1 1 -1), were collected (both considered respect to the 0.5860 nm cubic cell parameter).

With the available resolution and statistics, no atomic order changes could be assessed in the two experiments performed, but slight peak position changes could be detected for some peaks (see fig. 4 C), showing a temporal structural effect. These changes are correlated with the electrical resistance evolution after the temperature step (fig. 4 D). The structural evolution might be related to small atomic order rearrangements or to vacancies (or to vacancy aggregates) moving collectively to the surface of the sample.

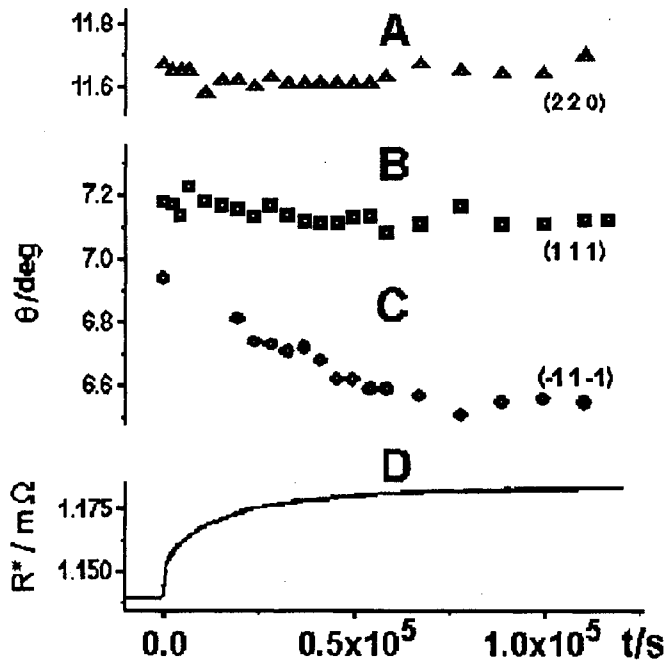


Figure 4. Structural effects of time and temperature (single crystal composition b): Position of neutron diffraction peaks versus time after a temperature step (from 293 K to 339 K). A: (2 2 0). B: (1 1 1). C: (-1 1 -1). D: reduced resistance R^* versus time in a similar sample. Bottom: Resistance evolution in a longer time scale.

4. CONCLUSIONS

High resolution detailed measurements allow the detection and characterization of the evolutive patterns in SMA. The electrical resistance provides a parameter representative of the evolution of the state of the material.

The strong after quench effects proceeds much faster (times around few days) than "stationary" long-time effects (months at room temperatures). The after quench effects should be related to the excess vacancies present after the quench, modifying slightly the atomic ordering conditions as a function of time. However, some after quench effects remain for a considerable long time, and may be revealed by a slight temperature increase.

After full homogeneization, or long time after the quench, temperature and time effects can be well described by two thermally activated processes, with activation energies slightly higher than the ones corresponding to vacancies. Atomic ordering or vacancy associations might be responsible for these effects, which relate directly to Ms changes with room temperature and time. It was possible to establish a model, which allowed the computation of Ms changes from the temperature evolution, with results in good agreement to the experimental Ms determinations.

The macroscopic high resolution measurements, as resistance versus time and temperature, allowed establishing the time scales where to look for the structural changes in the material. Small atomic ordering changes seem to exist after the quench. After a temperature step, slight diffraction peaks position changes could be detected, suggesting the development of a temporal monoclinic distortion. These changes are correlated with the electrical resistance evolution after the temperature step. The structural evolution might be related to small atomic order rearrangements or to vacancies (or vacancy aggregates) moving collectively to the surface of the sample.

Acknowledgements

M.T. Fernandez-Diaz helped with the neutron diffraction as a local contact, which was performed on the frame of the ILL experiment number 5-15-458 (1999). Fruitful discussions and help with the preparation of the samples are acknowledged from Dr. F.C. Lovey and Dr. J.L. Pelegrina (División Metales, C. A. Bariloche).

References

- [1] CM. Wayman: MRS Bulletin 18 (1993), p. 49-56
- [2] M. Ahlers: Prog. Mater. Sci. 30 (1986), p. 135-186
- [3] L. Buffard, Ecole Centrale de Lyon (France) Doctoral Thesis, (1991) (in french)
- [4] F. C. Lovey, V. Torra: Prog. Mater. Sci. 44 (1999), p. 189-289
- [5] A. Isalgue and V. Torra: J. Physique IV, 7 (1997), p. C5-339 C5-344.
- [6] A. Isalgue and V. Torra: J. of Thermal Anal. 52 (1998), p. 773-780
- [7] A. Isalgue, J.L. Pelegrina, A. Torralba, V.R. Torra, V. Torra: In: L.C. Brinson and B. Moran eds., Mechanics of phase transformations and shape memory alloys, ASME, AMD, vol. 189 (1994) p. 71-84
- [8] A. Isalgue, V. Torra: Meas. Sci. Technol. 4 (1993), p. 456-459
- [9] V. Torra and A. Isalgue: "Dynamic Effects in Cu-Zn-Al Shape Memory Alloys", in Solid-solid Phase Transformations II, PTM'99, The Japan Institute of Metals (1999) Kyoto, Japan, M. Koiwa K. Otsuka, T. Miyazaki eds, p.867-870
- [10] F.C. Lovey, A. Isalgue, V. Torra: Acta Metall. Mater. 40 (1992) p. 3389-3394
- [11] A. Planes, L.I. Manosa, E. Vives, J. Rodriguez-Carvajal, M. Morin, G. Guenin, J.L. Macqueron: J. Phys.: Condensed Matter 4 (1992) 553-559
- [12] T. Tadaki, Y. Nakata, K. Shimizu: J. Physique IV 5 (1995), p. C8-81 - C8-90
- [13] T. Ohba, T. Finlayson, K. Otsuka: J. de Physique IV, 5 (1995) C8-1083 a C8-1086
- [14] A. Isalgue, J.L. Pelegrina, V. Torra: J. Thermal Anal. 53 (1998) p. 671-683
- [15] X. Ren, K. Otsuka: Nature 389 (1997), p. 579-582
- [16] R.W. Cahn: Nature 389 (1997), p. 121